Autosoliton propagation and mapping problem in optical fiber lines with lumped nonlinear devices

S. Boscolo,* S. A. Derevyanko, and S. K. Turitsyn
Photonics Research Group, School of Engineering and Applied Science, Aston University, Birmingham B4 7ET, United Kingdom

A. S. Kovalev and M. M. Bogdan
B. I. Verkin Institute for Low Temperature Physics and Technology, 47 Lenin Ave, 61103 Kharkov, Ukraine
(Received 2 November 2004; published 1 July 2005)

A theoretical model is developed to describe the propagation of ultrashort optical pulses in fiber transmission systems in the quasilinear regime, with periodically inserted in-line nonlinear optical devices.

DOI: 10.1103/PhysRevE.72.016601 PACS number(s): 42.81.Dp, 42.81.Wg

INTRODUCTION

Efficient growth of the capacity of digital communication systems can be achieved by increase of the channel bit rate—the speed at which information symbols are transmitted. Increasing the channel rate assumes the utilization of shorter time slots allocated for each information bit and, consequently, of shorter carrier pulses. The propagation of ultrashort pulses is strongly affected by the fiber dispersion, which results in large temporal broadening of the carrier pulses. Because of the temporal broadening during propagation, the carrier pulse power spreads over many time slots and, consequently, the accumulated effect of the instantaneous fiber nonlinearity tends to get averaged out. Signal transmission using very short optical pulses is often referred to as the quasilinear regime [1]. This regime is, in some sense, opposite to soliton [2] or dispersion-managed (DM) soliton [3] transmission, where fiber nonlinearity plays an important role in preserving the pulse shapes during propagation. Note that in the quasilinear regime, the in-line Kerr nonlinearity is almost a "negative" factor contributing to the destabilization and distortion of carrier pulses. Therefore a certain amount of "constructive" nonlinearity is required to stabilize ultrashort pulse propagation and thus to improve the system performance. Recently, the periodic in-line deployment of nonlinear optical devices (NODs), such as nonlinear optical loop mirrors (NOLMs), semiconductor saturable absorbers, and semiconductor amplifier-based devices, has been demonstrated to be an effective technique of all-optical signal regeneration [4–6], which may achieve stable pulse propagation and virtually unlimited transmission distances in high-speed, strongly DM optical fiber communication systems [5]. It has numerically been shown in Refs. [4,5] that, under certain conditions, the interplay between fiber dispersion, the lumped nonlinearity provided by in-line NOLMs, and the action of linear control elements, such as optical filters, leads to the formation of autosolitons, which are periodically reproduced at the output of each segment of the transmission line. The term "autosolitons" here means robust localized pulses with the parameters prescribed by properties of the system, which occur in models combining conservative and dissipative dispersive and nonlinear terms [7–11].

The use of ultrashort optical pulses in fiber-optic communication leads to interesting physical regimes and different mathematical models should be introduced to adequately describe such transmission systems. In this paper a theory is developed to describe the optical signal transmission in DM fiber transmission systems in the quasilinear regime, with periodically in-line placed point NODs. We present a fundamental discrete mapping equation governing the carrier pulse propagation in a unit cell of the transmission line. As a particular sample approach to the solution of this basic model, we apply a variational method to determine the steady state pulse characteristics. Without loss of generality, as a specific practical application of the general theory, we consider a system with in-line NOLMs.

THEORETICAL MODEL

The optical pulse propagation in a cascaded transmission system with periodic variations of dispersion and nonlinearity, frequency filtering, and NOD management can be described by

$$i\frac{\partial E}{\partial z}-\frac{1}{2}\beta_2(z)\frac{\partial^2 E}{\partial t^2}+\sigma(z)|E|^2E=iG(z,|E|^2)E, \qquad (1)$$

where $E(z,t)$ is the slowly varying pulse envelope in the comoving system of coordinates, $\beta_2(z)$ represents the variation in the group-velocity dispersion due to dispersion compensation, and is assumed to be a periodic function of z with the period L, $\beta_2(z)=\beta_2(z+L)$, and σ is the fiber nonlinear coefficient. It is customary to express β_2 in terms of the associated dispersion coefficient D via $\beta_2=-\lambda^2 D/(2\pi c_0)$, where λ is the carrier wavelength, c_0 is the speed of light, and D is measured in ps/(nm km). Function $G(z,|E|^2)$ accounts for the signal attenuation due to fiber loss, the signal amplification by optical amplifiers, the action of filters, and the nonlinear gain at the NODs, and can be presented as

*Electronic address: boscolsa@aston.ac.uk

$$G(z,|E|^2) = -\gamma(z) + \sum_k \delta(z-kZ_a)\{\exp[\int_{(k-1)Z_a}^{kZ_a} dz\, \gamma(z)] - 1\} + \sum_k \delta(z-kZ_f)[h(t) * -1] + \sum_k \delta(z-kZ_0) \times [f(|E|^2) - 1]. \quad (2)$$

In Eq. (2), we have assumed that amplifiers, filters, and NODs are placed periodically in the system with the respective periods Z_a, Z_f, and Z_0. $\gamma = 0.05\ln(10)\alpha$ is the fiber loss coefficient that accounts for the signal attenuation along the fiber span before the kth amplifier, α is given in dB/km, and $\exp[\int_{(k-1)Z_a}^{kZ_a} dz\, \gamma(z)] - 1$ is the amplification coefficient after the fiber span between the $(k-1)$th and kth amplifiers. $h(t)$ is the inverse Fourier transform of the filter transfer function, and $*$ represents the Fourier convolution. The NODs are specified by their power-dependent transfer function $f(P)$. Hereafter, we will focus on loss (gain)-unbalanced fiber NOLMs. The transfer function for such devices can be written in the form

$$f(P) = a\sin(bP)\exp(icP), \quad (3)$$

with $a,b,c \in \Re^+$ some given constants.

To simplify the full model given by system (1), we make some justified physical assumptions. Here, we analyze the case of linear propagation in fiber, when we can neglect the nonlinear term in Eq. (1). Such a propagation regime corresponds to the case when the nonlinear length $L_{\mathrm{NL}} = (\sigma P_0)^{-1}$ (P_0 is the signal peak power) in the fiber is much larger than the local dispersion length $L_{\mathrm{D}} = T^2/|\beta_2|$ (T is the pulse width). The transformation of a pulse after propagation in one segment of the transmission line can be considered as the mapping of the input pulse into the output one. If we consider an element of the transmission line that includes a NOD given by Eq. (3), a piece of linear fiber of length Z_0, and m filters, the mapping of the signal, defined up to a phase factor μ, can be presented as

$$e^{i\mu}U_{n+1}(t) = \int_{-\infty}^{+\infty} dt'\, K(t-t';Z_0) f(|U_n(t')|^2) \times U_n(t'), \quad n = 0,1,\ldots. \quad (4)$$

The derived equation is one of the central results of the paper. This mapping problem plays a fundamental role in the description of fiber communication systems at high bit rates. To obtain Eq. (4), we have assumed that each NOD is placed immediately after an amplifier, and we have applied the transformation $U(z,t) = Q^{-1}(z)E(z,t)$, where $Q(z) = \exp[-\int_{(k-1)Z_a}^{z} dz'\, \gamma(z')]$ for $(k-1)Z_a < z < kZ_a$, and $Q(z) = 1$ for $z = kZ_a^+$. In Eq. (4), the signal is taken at the input point nZ_0^- to the NOD after any device prior to the NOD. The kernel K describes the signal propagation in the unit cell Z_0. In the case when Gaussian filters are used, K can be written in the form

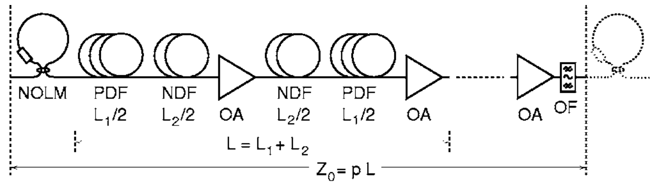

FIG. 1. One element of the periodic transmission system.

$$K(t-t';Z_0) = \sqrt{G}\sqrt{\frac{i}{2\pi(B_0 + im/\Omega_f^2)}} \times \exp\left[-\frac{i(t-t')^2}{2(B_0 + im/\Omega_f^2)}\right], \quad (5)$$

where $\Omega_f = \pi\delta\nu_f/\sqrt{\ln 2}$ is the filter bandwidth [$\delta\nu_f$ denotes the full width at half maximum (FWHM) bandwidth], and $B_0 = \int_{nZ_0}^{(n+1)Z_0} dz\, \beta_2(z)$ is the total accumulated dispersion. In Eq. (5), the excess gain G accounts for compensation of the signal energy losses introduced by the NODs and filters in the system. From the transmission point of view it is desirable to find (if exists) a steady state propagation regime in which an optical pulse propagating along the transmission line reproduces periodically at the output of each element of the line. That corresponds to determining a fixed point of mapping (4). Therefore in order to find the steady state pulse shape $U(t)$, one has to solve a nonlinear integral equation, which stems from Eq. (4) if we put $U_{n+1}(t) = U_n(t) = U(t)$. If the steady state pulse is stable, then any initial signal within the basin of attraction of the fixed point will gradually evolve towards it after some maps.

AUTOSOLITON STRUCTURES

In this section, we demonstrate the feasibility of stable autosoliton propagation guided by in-line NOLMs, by direct numerical simulations of the basic propagation model [Eq. (1)]. The sample transmission scheme used in the numerical integration of Eq. (1) is depicted in Fig. 1. The transmission line is composed of an equal number of positive (anomalous) dispersion fiber (PDF) segments and negative (normal) dispersion fiber (NDF) segments. The dispersion map consists of an alternation of a PDF-NDF block and a mirror NDF-PDF block. Fiber parameters of practical importance are used for the PDF and the NDF [5]. We note that fiber nonlinearity is included in the calculations. An optical amplifier (OA), which compensates for the fiber loss, follows each of the two blocks. The high values of the local dispersion of the fibers together with the short pulse widths that are typically used to operate the system at high data transmission rates result in large broadening of the pulses during propagation. These regimes are beyond the range where stable propagation of DM solitons has been observed [12]. A NOLM is placed into the transmission line every an integer number p of dispersion map periods, $Z_0 = pL$. We note that in this case $B_0 = \langle\beta_2\rangle Z_0 = -\lambda^2\langle D\rangle Z_0/(2\pi c_0)$ ($\langle\cdot\rangle$ denotes the average over the dispersion compensating period L). In the sample configuration used here, $Z_0 = 391$ km, and $p = 5$. A single ($m = 1$) Gaussian optical filter (OF) is placed after the amplifier

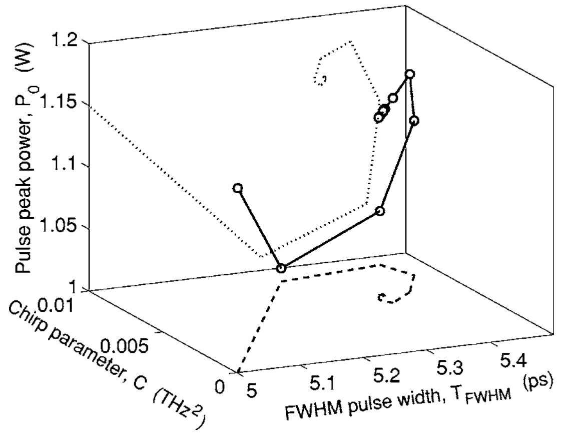

FIG. 2. Acquisition of the steady state in the space FWHM pulse-width-chirp-parameter-peak power as viewed at the NOLM input.

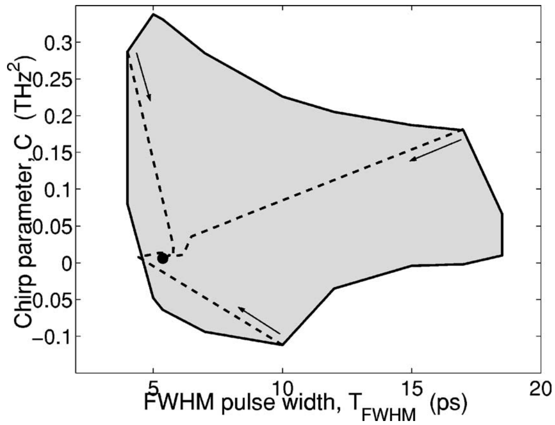

FIG. 3. Basin of attraction of the steady state solution of Fig. 2 in the plane FWHM pulse-width-chirp parameter.

prior to the NOLM location. The loss-unbalanced NOLM configuration is employed as an example, and preamplification of the input pulses to the NOLM is used (see Ref. [5] for details). Parameters a, b, and c in Eq. (3) have the respective values: 0.06369, 1.823, and 1.839. Following Ref. [5], the system is operated such that the peak power of the steady state pulses (if any exist) is in the region slightly past the first peak of the continuous-wave power characteristic of the NOLM.

Figure 2 shows an example of the evolution of the pulse parameters in the system, measured stroboscopically at the NOLM input point. In this example, an unchirped Gaussian pulse is launched into the system, with the peak power $P_0 = 1.15$ W (corresponding to 3.5 mW at the starting point of the transmission) and the FWHM pulse width $T_{\mathrm{FWHM}}=5$ ps. The system parameters are $\langle D\rangle = 0.009$ ps/(nm km), $\delta\nu_f = \sqrt{\ln 2}\Omega_f/\pi = 0.1$ THz, and $G=627.0$ (28.0 dB). The pulse chirp parameter is calculated as $C = \mathrm{Im}\int_{-\infty}^{+\infty} dt\, U^2(U_t^*)^2 / \int_{-\infty}^{+\infty} dt|U|^4$. One may see from Fig. 2 that the pulse parameters converge to a steady state after a short initial transient. This result demonstrates the feasibility of stable pulse propagation in the system, and indicates that the use of in-line NOLMs converts the quasilinear transmission regime into an autosoliton transmission regime, which is strictly nonlinear [5]. We note that the same stroboscopic picture as that in Fig. 2 can be obtained by simply iterating mapping equation (4). Figure 3 shows the basin of attraction of the steady state solution of Fig. 2 in the plane (T_{FWHM}, C). To calculate Fig. 3, the initial pulse peak power has been set to its steady state value. It is seen that there is a large tolerance to the initial pulse width and chirp, which indicates a high degree of stability of the steady state solution. We have also defined the tolerable limits of the stable pulse propagation to the filter bandwidth and the path-averaged dispersion of the line. The results are shown in Fig. 4, where $\delta\nu_f$ and $\langle D\rangle$ are varied within a practical range of values. In Fig. 4, the excess gain G is chosen such that the stationary pulse peak power is approximately 1.15 W at the NOLM input.

SIMPLE APPROXIMATE APPROACH

As we pointed out previously, in order to find a steady state pulse propagation regime, one has to solve mapping integral equation (4) for the fixed points. While this can be done numerically, for massive optimization of the system parameters it is very useful to have a simplified approximate method to find solutions of the basic model. Therefore here we apply a simple variational approach. We noticed from full numerics that the steady state pulse shape at the NOLM input point can always be fitted well by a Gaussian profile. Thus we choose a trial input pulse $U(t)$ for the map as a Gaussian-shaped pulse with (yet unknown) peak power P_0, root-mean-square (RMS) width T_{RMS}, and RMS chirp parameter C_{RMS}: $U_n(t) = \sqrt{P_0}\exp[-t^2/(4T_{\mathrm{RMS}}^2) + iC_{\mathrm{RMS}}t^2]$. The output of the map $U_{n+1}(t)$ given by Eq. (4) will be non-Gaussian in general, but will have a close shape and will depend on the parameters of the input signal, $U_{n+1} = U_{n+1}(t; P_0, T_{\mathrm{RMS}}, C_{\mathrm{RMS}})$. Let us now demand that the peak power, pulse width, and chirp of the output signal coincide with those of the input Gaussian signal. This provides a system of transcendental equations for the sought parameters P_0, T_{RMS}, and C_{RMS},

$$P_0 = \frac{1}{\sqrt{2\pi}T_{\mathrm{RMS}}}\int_{-\infty}^{+\infty} dt |U_{n+1}(t; P_0, T_{\mathrm{RMS}}, C_{\mathrm{RMS}})|^2,$$

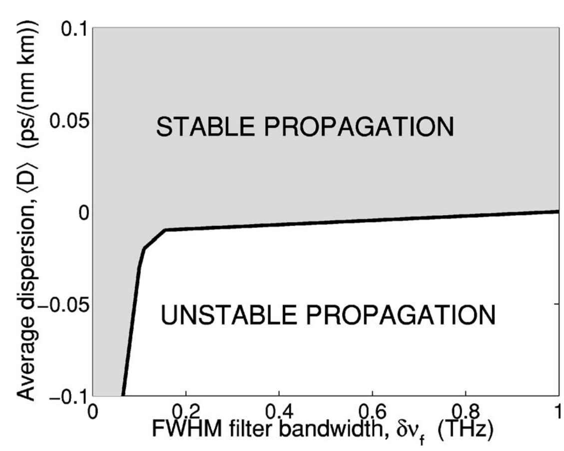

FIG. 4. Limits of stable pulse propagation in the plane filter bandwidth-average dispersion.

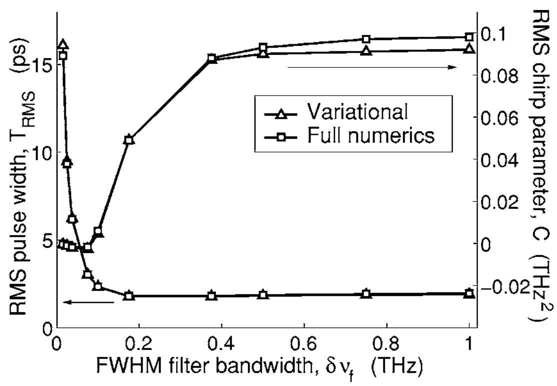

FIG. 5. Steady state RMS pulse width (left axis) and RMS chirp parameter (right axis) at the NOLM input versus filter bandwidth.

$$T_{\mathrm{RMS}}^2 = \frac{\displaystyle\int_{-\infty}^{+\infty} dt\, t^2 |U_{n+1}(t;P_0,T_{\mathrm{RMS}},C_{\mathrm{RMS}})|^2}{\displaystyle\int_{-\infty}^{+\infty} dt |U_{n+1}(t;P_0,T_{\mathrm{RMS}},C_{\mathrm{RMS}})|^2},$$

$$\begin{aligned} C_{\mathrm{RMS}} = \mathrm{Im}\int_{-\infty}^{+\infty} dt\, U_{n+1}^2(t;P_0,T_{\mathrm{RMS}},C_{\mathrm{RMS}}) \\ \times [\partial_t U_{n+1}^*(t;P_0,T_{\mathrm{RMS}},C_{\mathrm{RMS}})]^2 \\ \times \left[\int_{-\infty}^{+\infty} dt |U_{n+1}(t;P_0,T_{\mathrm{RMS}},C_{\mathrm{RMS}})|^4\right]^{-1}. \end{aligned} \quad (6)$$

If the solution of system (6) exists, then it provides a variational approximation for the parameters of the steady state pulse. In particular, one may use the Gaussian ansatz with the found vaues of P_0, T_{RMS}, and C_{RMS} as an approximation of the steady state pulse shape.

The theoretical predictions from the variational model [Eqs. (6)] have been compared with the results of full numerical simulations. The steady state RMS pulse width and RMS chirp parameter are plotted in Fig. 5 as a function of the filter bandwidth, for $\langle D\rangle = 0.009$ ps/(nm km), and the same values of G as used in Fig. 4. The steady state intensity profile and chirp (first time derivative of the phase) of the input pulse to the NOLM are plotted in Fig. 6, for $\delta\nu_f = 0.1$ THz. It can be seen that the results from the variational model are in good agreement with the simulation results.

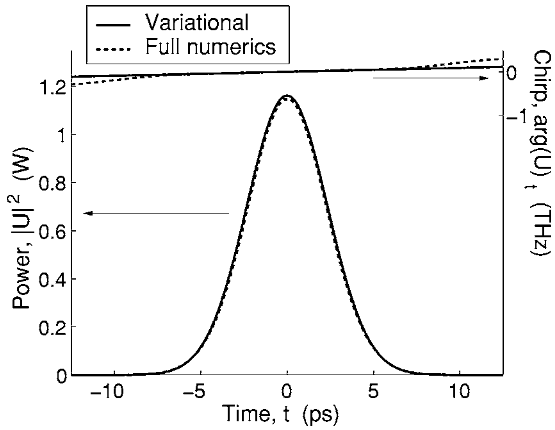

FIG. 6. Intensity (left axis) and chirp (right axis) of the steady state pulse at the NOLM input.

CONCLUSION

We have developed a theoretical model to describe the ultrashort pulse propagation in fiber transmission systems in the quasilinear regime, with periodic in-line deployment of NODs. In the particular application with NOLMs, we have numerically demonstrated that formation of autosolitons can be observed in such systems, as a result of a balance between the effects of dispersion in the transmission fibers, linear control by optical filters, and nonlinear focusing in the NOLMs. A variational principle has been applied to determine the steady state pulse characteristics, and the theoretical analysis has been shown to accurately reproduce the results of full numerical simulations.

ACKNOWLEDGMENTS

This work was partially supported by Leverhulme Trust Project No. F/00250/B and NATO Collaborative Linkage Program No. PST.CLG.980068.

[1] P. V. Mamyshev and N. A. Mamysheva, Opt. Lett. **24**, 1454 (1999).
[2] A. Hasegawa and Y. Kodama, *Solitons in Optical Communications* (Oxford University Press, Oxford, 1995).
[3] I. Gabitov and S. K. Turitsyn, Opt. Lett. **21**, 327 (1996).
[4] S. Boscolo, J. H. B. Nijhof, and S. K. Turitsyn, Opt. Lett. **25**, 1240 (2000).
[5] S. Boscolo, S. K. Turitsyn, and K. J. Blow, IEEE Photonics Technol. Lett. **14**, 30 (2002).
[6] D. Rouvillain *et al.*, Electron. Lett. **38**, 1113 (2002).
[7] B. S. Kerner and V. V. Osipov, *Autosolitons* (Kluwer Academic, Dordrecht, 1994).
[8] V. S. Grigoryan, Phys. Lett. A **149**, 371 (1990).
[9] A. G. Vladimirov, G. V. Khodova, and N. N. Rosanov, Phys. Rev. E **63**, 056607 (2001).
[10] I. Gabitov, D. D. Holm, B. P. Luce, and A. Mattheus, Opt. Lett. **20**, 2490 (1995).
[11] I. Gabitov, D. D. Holm, and B. P. Luce, J. Opt. Soc. Am. B **14**, 1850 (1997).
[12] J. H. B. Nijhof, N. J. Doran, W. Forysiak, and A. Berntson, Electron. Lett. **34**, 481 (1998).